ELSEVIER

Chemical Engineering Science 61 (2006) 7421–7435

Chemical Engineering Science

www.elsevier.com/locate/ces

# Self-similar inverse population balance modeling for turbulently prepared batch emulsions: Sensitivity to measurement errors

Neha B. Raikar, Surita R. Bhatia, Michael F. Malone, Michael A. Henson*

*Department of Chemical Engineering, University of Massachusetts, Amherst, MA 01003-9303, USA*

Received 10 March 2006; received in revised form 18 July 2006; accepted 7 August 2006
Available online 25 August 2006

**Abstract**

We investigate the sensitivity of an inverse population balance equation (PBE) modeling technique for extracting single particle functions from transient size distribution measurements. A dynamic PBE model of a turbulently agitated batch emulsification vessel is used to generate volume size distribution data under the assumption of negligible drop coalescence. The distribution data are subjected to various types of error consistent with available measurement technologies and then introduced as input data to the inverse PBE modeling algorithm, which includes validation of the self-similar assumption. The errors considered include measurement noise, data skewed towards smaller or larger drops, skewed data due to the presence of large dust peaks, and reduced resolution caused by data binning. For each case, the computed functions for the drop breakage rate and the distribution of daughter drops are compared to the actual functions to assess the impact of input data errors on the effectiveness of the inverse PBE modeling approach. The type of measurement errors considered generally lead to underprediction of the breakage rate and, consequently, to overprediction of the number of large drops. Because the estimated and actual breakage rates tend to converge at small drop sizes, the inverse algorithm generates accurate predictions of the drop size distribution at sufficiently long batch times when small drops dominate. Implications for our future work on PBE modeling of drop size distributions in pharmaceutical emulsions prepared with high pressure homogenization are discussed.


*Keywords:* Emulsions; Drop size distributions; Population balance equation models; Inverse problem

## 1. Introduction

Particulate systems are ubiquitous in the agricultural, chemical, polymer, food and beverage, consumer products and pharmaceutical industries. Emulsions are common dispersed phase systems with diverse applications that include processed foods, polishes, waxes, agricultural sprays and road surfacing (Becher, 2001, Chapter 8). We are particularly interested in pharmaceutical applications where hydrophobic drugs are encapsulated in oil-in-water emulsions and delivered to patients via oral administration, parenteral delivery, ophthalmic medicine, and topical and transdermal creams (Marti-Mestres and Nielloud, 2002). Important criteria for the formulation of pharmaceutical emulsions include biocompatibility, biodegradability, toxicity, and targeting to specific organs and tissues to improve drug effectiveness and reduce undesirable side effects. Thus, the drug properties, emulsion characteristics and administration route must be matched properly for each application (Nielloud and Marti-Mestres, 2000).

Pharmaceutical emulsions are often manufactured by subjecting a coarse emulsion containing a small molecule, hydrophobic drug to high pressure homogenization where the dispersion is forced through a small orifice under very high pressure. The homogenization process produces an emulsion with a distribution of drop sizes that is determined by the chemical formulation, the initial coarse distribution, and the homogenizer operating conditions (Becher, 1983, Chapter 2; Floury et al., 2004a,b; Soon et al., 2001; Walstra, 1993). Like other particulate systems, the final properties of a pharmaceutical emulsion are a complex and often unknown function of many different variables. Clinical studies have shown that the drop size distribution has a significant impact on emulsion

* Corresponding author. Tel.: +1 413 545 3481; fax: +1 413 545 1647.
*E-mail address:* henson@ecs.umass.edu (M.A. Henson).

0009-2509/$ - see front matter © 2006 Elsevier Ltd. All rights reserved.
doi:10.1016/j.ces.2006.08.022

properties and the ultimate effectiveness of the drug delivery system (Malmsten, 2002). For example, the biodistribution of the encapsulated drug is strongly affected by drop size as well as complex physiological processes (Nielloud and Marti-Mestres, 2000, Chapter 5). In addition to exhibiting long-term stability and producing the desired drug release kinetics, the emulsion should usually be nearly monodisperse with a mean drop size chosen to target specific tissues and organs.

The population balance equation (PBE) modeling framework has been used to describe the evolution of the particle size distribution in systems ranging from liquid–liquid dispersions to microbial cell populations (Alexopoulos and Kiparissides, 2005; Alexopoulos et al., 2004; Chen et al., 1998; Coulaloglou and Tavlarides, 1977; Kostoglou et al., 1997; Kostoglou and Karabelas, 1997; Ramkrishna, 2000). Representative applications of PBE modeling to dispersed phase systems include the description of drop interaction processes in continuously agitated liquid–liquid dispersions (Alopaeus et al., 1999, 2002, 2003; Coulaloglou and Tavlarides, 1977; Kostoglou and Karabelas, 2001; Sovova, 1981; Sovova and Prochazka, 1981), the simulation of drop size distributions for liquid–liquid extractors (Ruiz et al., 2002; Ruiz and Padilla, 2004; Simon et al., 2003), the prediction of drop size distributions in a continuous flow screw-loop reactor (Chen et al., 1998), simulation of bubble size distributions (Wang et al., 2006) and the emulsification of coarse suspensions or formation of small vesicles in ultra-high velocity jet homogenizers (Maguire et al., 2003; Soon et al., 2001). Successful application of the PBE modeling approach requires knowledge of functions for phenomena such as particle formation, aggregation, and breakup (Chen et al., 1998; Coulaloglou and Tavlarides, 1977; Ramkrishna, 2000; Ruiz and Padilla, 2004; Tsouris and Tavlarides, 1994). Because functions that accurately predict experimental data are difficult to develop from fundamental principles, several inverse PBE techniques for extracting the single particle functions from particle distribution data have been developed (Kostoglou et al., 1997; Kostoglou and Karabelas, 2005; Mahoney et al., 2002; Sathyagal et al., 1995).

In this paper, we consider an inverse PBE modeling method developed by Ramkrishna (2000) and co-workers, which is based on the concept of self-similar solutions (Kumar and Ramkrishna, 1996a,b; Ramkrishna and Mahoney, 2002; Ramkrishna et al., 1995). Transient particle size distribution data are first tested for self-similarity, and then used for non-parametric reconstruction of the functions for drop breakup and the creation of daughter drops if the self-similarity property holds. This inverse PBE method has been applied to both simulated and experimental data for various dispersions prepared with turbulent agitation in well-mixed batch vessels (Narsimhan et al., 1980, 1984; Ramkrishna, 1974; Sathyagal and Ramkrishna, 1996; Sathyagal et al., 1995; Wright and Ramkrishna, 1992). Because different combinations of single drop functions can provide agreement with the limited transient drop size distribution data typically available for estimation, the inverse problem is inherently ill-posed (Ramkrishna, 2000). Consequently, function approximation results are expected to be highly sensitive to the quality and quantity of the input data.

Techniques for measuring emulsion drop size distributions include optical microscopy and various light scattering techniques. Dynamic light scattering (DLS) (Schmitz, 1990) allows for measurement of droplets in the 10–1000 nm range, and is ideal for many pharmaceutical applications that target droplets in the 100 nm range. These small droplets cannot be observed by optical microscopy. In addition, DLS enables much larger sample volumes to be probed than is possible using optical microscopy. However, DLS measurements are subject to various errors that degrade data quality like sensor noise. Because larger drops scatter more strongly than small drops, DLS has a tendency to skew the size distribution towards larger drops. Dust particles can introduce artificial peaks at large drop sizes that may be difficult to remove. Automated signal filtering can inadvertently remove signals associated with large droplets, while emulsion sample filtering can induce changes in the drop size distribution due to shearing. The calculation of the autocorrelation function and subsequent inversion to produce the particle size distribution involves binning operations that reduce resolution. While numerous application studies of the inverse PBE approach have been reported, we are not aware of any investigations focusing on the effects of such input data errors.

In this paper, we utilize a previously published model of a well-mixed batch emulsification vessel (Sathyagal et al., 1995) to examine the effect of transient drop size distribution measurement errors on the quality of the function approximation results obtained with the inverse PBE method of Ramkrishna and co-workers. The remainder of the paper is organized as follows. The PBE model and the inverse PBE method are described in Sections 2 and 3, respectively. New results on the sensitivity of the PBE method to input data errors are presented and discussed in Section 4. Finally, we summarize our main findings and discuss their implications for PBE modeling of drop size distributions in pharmaceutical emulsions prepared with high pressure homogenization in Section 5.

## 2. PBE model

The PBE describes the evolution of the drop size distribution that results from particulate processes such as formation, aggregation and breakup. We utilize a volume structure model in which drops are characterized by their volume. The population balance requires that for any volume element $\mathrm{d}v$, the number of drops moving in and out of the element are balanced by drops accumulating within the element. Let $n(v,t)\,\mathrm{d}v$ represent the number of drops per unit volume of the dispersion at time $t$ with volumes between $v$ and $v+\mathrm{d}v$. We neglect drop coalescence by assuming a small dispersed phase volume fraction and the presence of large amount of surfactant.

This formulation yields the following PBE for a well-mixed, batch vessel (Coulaloglou and Tavlarides, 1977; Ramkrishna, 2000):

$$\frac{\mathrm{d}n(v,t)}{\mathrm{d}t} = -\Gamma(v)n(v,t) + \int_v^\infty \beta(v,v')v(v')\Gamma(v')n(v',t)\,\mathrm{d}v', \tag{1}$$

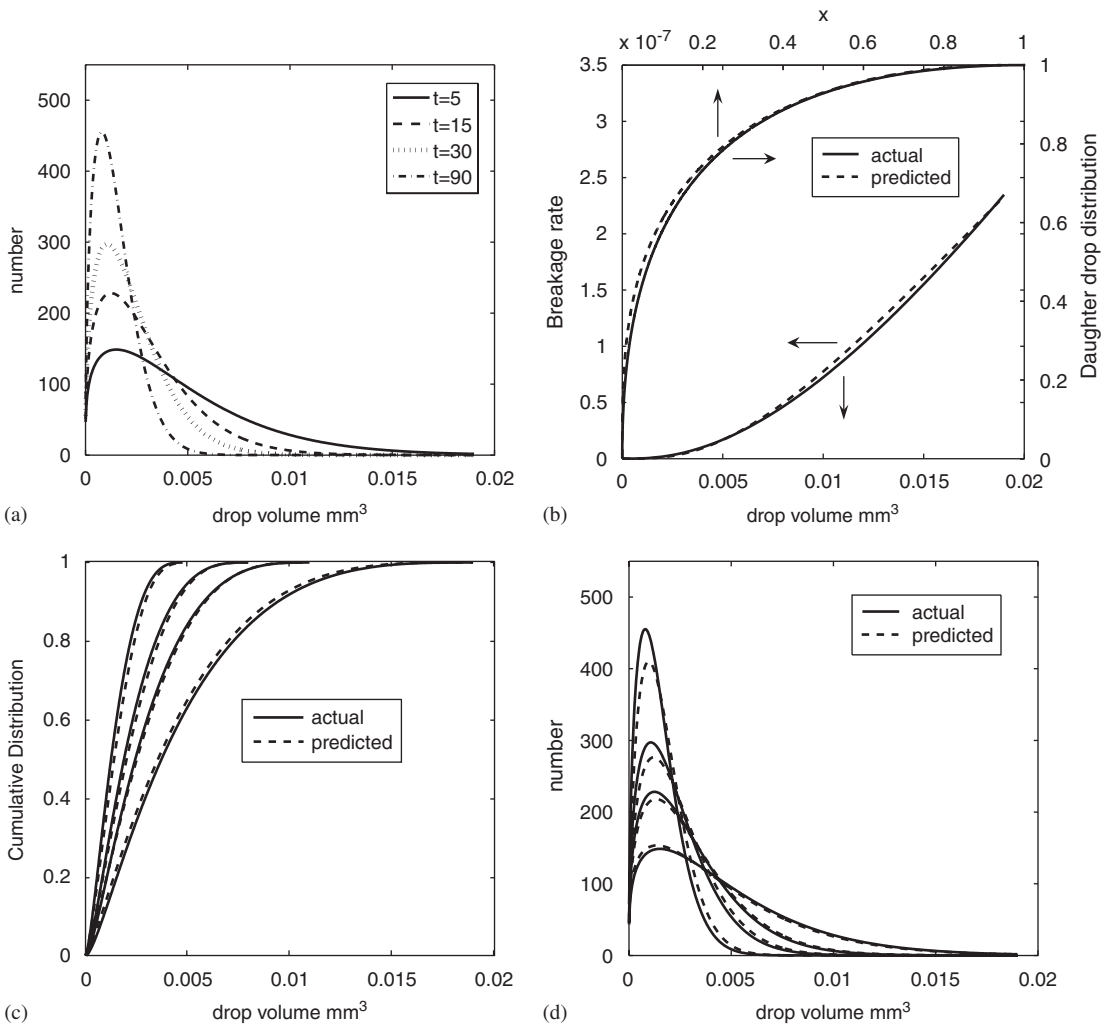


Fig. 1. Inverse population balance modeling results for perfect drop volume distribution data. (a) Transient number drop distributions. (b) Predicted and actual drop breakage rate and daughter drop distribution functions. (c) Predicted and actual transient cumulative drop distributions. (d) Predicted and actual transient number drop distributions.

where $\Gamma(v)$ is the breakage rate (fraction of drops of volume $v$ breaking per unit time), $\beta(v, v')$ is the probability density function (probability of forming drops of volume $v$ from breakage of drops of volume $v'$), and $\nu(v')$ is the number of daughter drops formed by breakage of drop of volume $v'$. The initial condition $n(v, 0)$ is the number density of the coarse emulsion introduced to the vessel and can be measured experimentally.

For application of the inverse modeling approach of Ramkrishna and co-workers (Ramkrishna, 2000), the PBE model is conveniently reformulated in terms of the cumulative distribution rather than the number distribution as in (1). In this case, the PBE for a pure breakage process assumes the form:

$$\frac{\partial F(v,t)}{\partial t} = \int_0^\infty \Gamma(v')G(v,v')\partial_v F(v',t), \tag{2}$$

where $F(v, t)$ is the cumulative volume fraction of drops of volume less than or equal to $v$ at time $t$, $\Gamma(v)$ is the breakage rate of drops of volume $v$, and $G(v, v')$ is the cumulative volume fraction of drops of volume less than or equal to $v$ formed by breakage of drop of volume $v'$. The function $G(v, v')$ combines the two functions $\beta(v, v')$ and $\nu(v')$ in (1).

The PBE model (2) is completed by specifying the breakage rate $\Gamma(v)$ and the daughter drop distribution function $G(v, v')$. A wide variety of functional forms have been proposed for dispersed phase systems (Ramkrishna, 2000). In this paper, we employ the functions introduced in Sathyagal et al. (1995) for drop breakage in a well-mixed dispersion. While these functions were not determined from experimental data, the inverse PBE method has been extensively studied for this problem under the assumption of perfect input data. We will utilize these results as the basis for assessing the impact of input data errors on the quality of the function approximation results. The breakage rate function used in our analysis has the form (Sathyagal et al., 1995):

$$\Gamma(v) = 1.2\exp[0.12(\ln v + 3.5) - 0.20(\ln v)^2 - 12.25]. \tag{3}$$

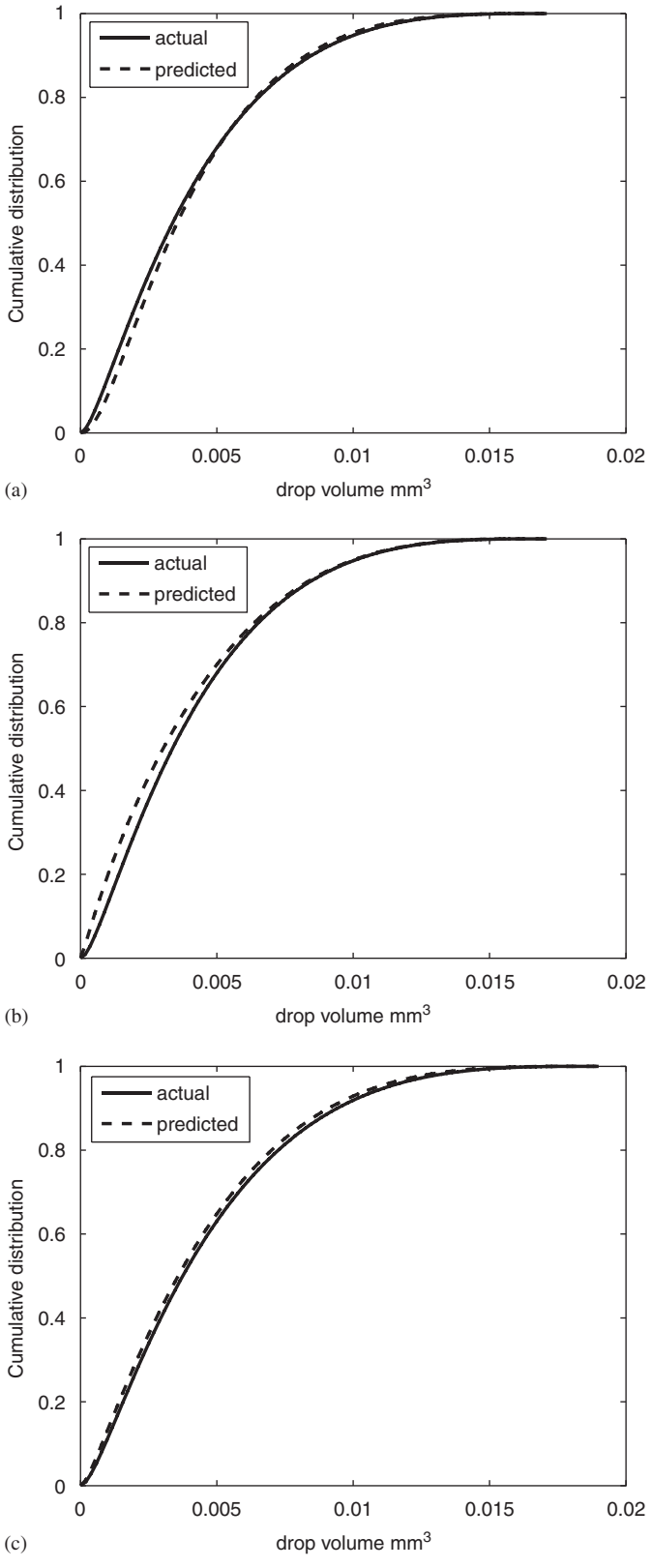


Fig. 2. Effect of the drop breakage and daughter drop distribution functions on the predicted cumulative distribution ($t = 5$ min). (a) Estimated breakage function and actual distribution function. (b) Actual breakage function and estimated distribution function. (c) Estimated breakage and distribution functions.

The assumption of self-similarity allows the daughter drop distribution function to be represented compactly as

$$G(v, v') = g(x) = g\left[\frac{\Gamma(v)}{\Gamma(v')}\right]. \tag{4}$$

We have used the following function in our analysis (Sathyagal et al., 1995):

$$g(x) = \tfrac{8}{3}\sqrt{x} - \tfrac{5}{3}x^{0.8}. \tag{5}$$

## 3. Inverse PBE modeling

The objective of the inverse PBE modeling approach of Ramkrishna and co-workers (Ramkrishna, 2000, Chapter 6) is to construct functions for single particle processes from transient measurements of the particle size distribution. A desirable feature of this methodology is that a priori specification of functional forms is not required. The concept of self-similarity is exploited repeatedly, starting with the assumption that the daughter drop distribution function can be represented as a function of the breakage rate function as in (4). While this functional form might appear to be highly restrictive, it subsumes power law relationships often used to describe drop breakage processes (Narsimhan et al., 1980; Sathyagal et al., 1995). The interested reader is referred elsewhere for a detailed treatment of self-similarity (Ramkrishna, 2000, Chapter 6). In this paper, we investigate approximation of the breakage rate function $\Gamma(v)$ and the daughter drop distribution function $g(x)$ from transient drop volume distributions obtained by simulating the PBE model (2) with the functions in (3) and (4). This simulation approach allows direct comparison of the approximated and actual functions to assess the impact of input data errors on the effectiveness of the inversion procedure.

### 3.1. Breakage rate function

The calculation of the breakage rate function requires testing of the similarity hypothesis and then determination of the breakage function if the similarity hypothesis is valid (Ramkrishna, 2000, Chapter 6; Sathyagal et al., 1995). Curves of $\ln t$ versus $\ln v$ are plotted for different values of the cumulative distribution $F$. The similarity property can be tested by evaluating the arc lengths of different $\ln t$ versus $\ln v$ curves using the following formula:

$$s(x) = \int_{x_0}^{x} \left[1 + \left(\frac{\mathrm{d}y}{\mathrm{d}x}\right)^2\right]^{1/2} \mathrm{d}x, \tag{6}$$

where $x = \ln v$ and $y = \ln t$. The arc length calculation requires evaluation and integration of the first derivative. If a single arc length curve is obtained from the different $\ln t$ versus $\ln v$ curves, then the data are self-similar. Typically, self-similarity is validated by visual inspection of the arc length curves. We found that each $\ln t$ versus $\ln v$ curve must be fit to a different linear or quadratic equation to obtain acceptable results.

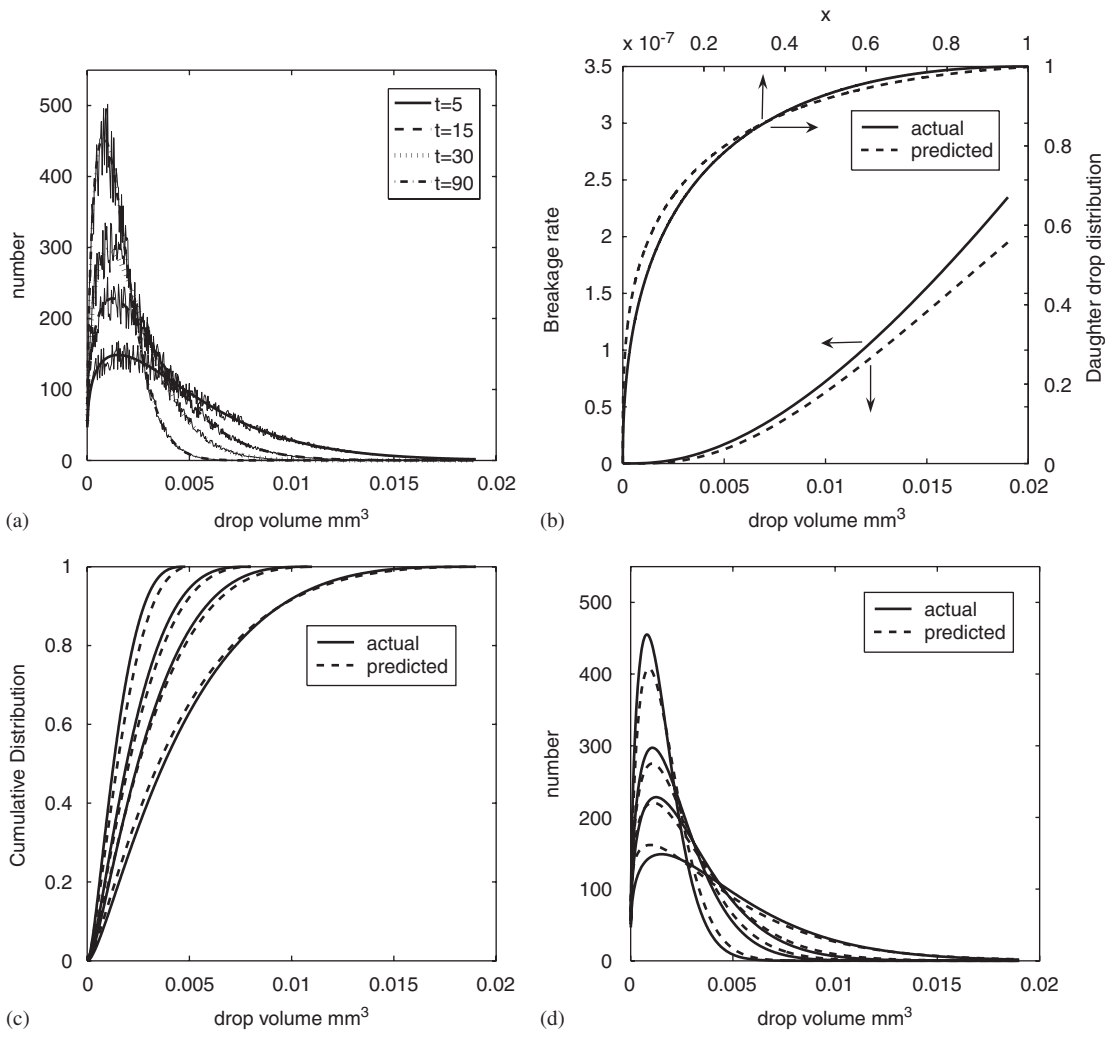


Fig. 3. Inverse population balance modeling results with six noisy drop volume distributions. (a) Noisy and actual transient number drop distributions. (b) Predicted and actual drop breakage rate and daughter drop distribution functions. (c) Predicted and actual transient cumulative drop distributions. (d) Predicted and actual transient number drop distributions.

From the arc length equation (6), a relation for the complete $\ln t$ versus $\ln v$ curve can be obtained:

$$\frac{\mathrm{d}\ln t}{\mathrm{d}\ln v} = \left[\left(\frac{\mathrm{d}s}{\mathrm{d}\ln v}\right)^2 - 1\right]^{1/2}. \tag{7}$$

This relation can be used to evaluate the partial derivative in the following equation, which allows calculation of the breakage function up to a multiplicative constant $\gamma$:

$$\Gamma(v) = \gamma \exp\left[-\int_{\ln v_0}^{\ln v}\left(\frac{\partial \ln t}{\partial \ln v}\right)_F \mathrm{d}\ln v\right], \tag{8}$$

where $\gamma$ is the breakage function evaluated at the reference volume $v_0$ used in the arc length calculations: $\gamma = \Gamma(v_0)$. The unknown constant $\gamma$ is determined as part of the procedure for approximating the daughter drop distribution function.

### 3.2. Daughter drop distribution function

The calculational procedure for the daughter drop distribution function utilizes the similarity variable defined as:

$$\xi = \frac{\Gamma(v)t}{\gamma}, \tag{9}$$

where the ratio $\Gamma(v)/\gamma$ is obtained from the breakage rate calculation (8). Application of the similarity transformation $F(v,t) \to f(\xi)$ to the cumulative form of the PBE (2) yields the following equation for the similarity distribution $\xi f'(\xi)$ (Ramkrishna, 2000; Sathyagal et al., 1995):

$$\xi f'(\xi) = \int_0^1 \frac{\xi^2}{x^3} f'\left(\frac{\xi}{x}\right) \gamma g(x)\,\mathrm{d}x, \tag{10}$$

where $x = \Gamma(v)/\Gamma(v')$ as in (4). This equation is the basis for determining the daughter drop distribution function $g(x)$ and the unknown breakage constant $\gamma$.

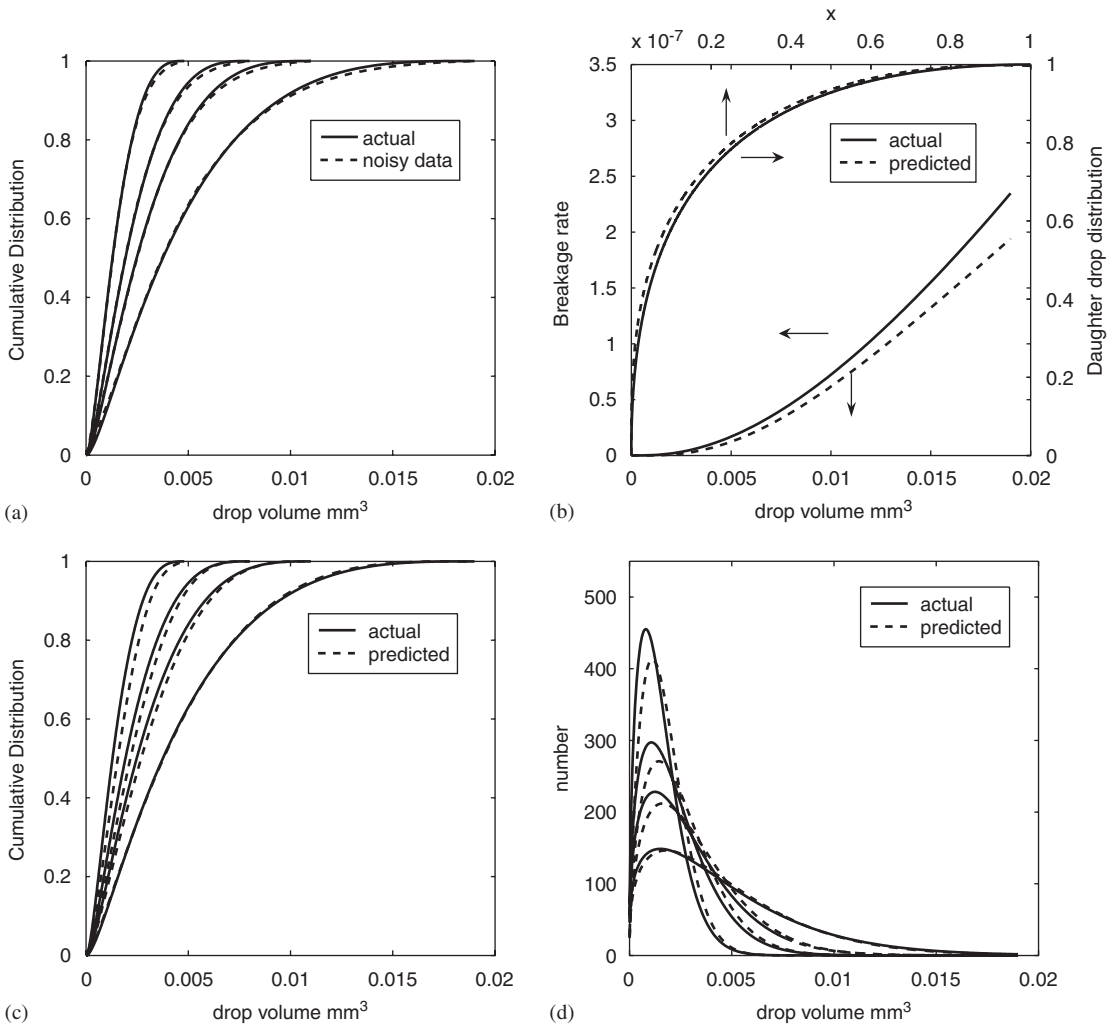


Fig. 4. Inverse population balance modeling results with twelve noisy drop volume distributions. (a) Noisy and actual transient cumulative drop distributions. (b) Predicted and actual drop breakage rate and daughter drop distribution functions. (c) Predicted and actual transient cumulative drop distributions. (d) Predicted and actual transient number drop distributions.

As suggested in Sathyagal et al. (1995), the unknown product $\gamma g(x)$ is expanded in terms of orthogonal basis functions chosen to be the modified Jacobi polynomials (Abramowitz and Stegun, 1964)

$$\gamma g(x) = \sum_{i=1}^{nb} a_j G_j(x) = \sum_{i=1}^{nb} a_j x^{\mu} J_j(x). \tag{11}$$

Three basis functions were used for our analysis. We found that $nb = 3$ was the minimum number of basis function required for approximating the distribution function without the need for regularization (Sathyagal et al., 1995). Because $\xi f'(\xi) \sim \xi^{\mu}$ for $\xi \approx 0$, the power $\mu$ can be obtained from the behavior of the self-similar distribution as $\xi \to 0$. We found that small, trial-and-error adjustments in this $\mu$ value may produce improved distribution predictions. Once the product $\gamma g(x)$ is determined via the procedure described below, the constant $\gamma$ is readily determined since $g(1) = 1$.

The similarity variable $\xi$ is discretized to generate $\{\xi_i\}$ and the matrix $X = \{X_{ij}\}$ associated with (10) is defined as

$$X_{ij} = \int_0^1 \frac{\xi_i^2}{x^3} f'\left(\frac{\xi_i}{x}\right) G_j(x)\,\mathrm{d}x. \tag{12}$$

As suggested in Sathyagal et al. (1995), the similarity distribution $\xi f'(\xi)$ was expanded in terms of gamma distributions:

$$\xi f'(\xi) = \sum_{k=1}^{n_{\text{term}}} A_k \xi^{\alpha_k - 1} \exp(-\beta_k \xi). \tag{13}$$

We used two-term expansions ($n_{\text{term}} = 2$) for our analysis. The unknown parameters ($A_k$, $\alpha_k$, $\beta_k$) of the expansion are determined from the known similarity distribution using nonlinear regression. By substituting the expansion (13) into (12) and performing the necessary integration, an explicit formula for

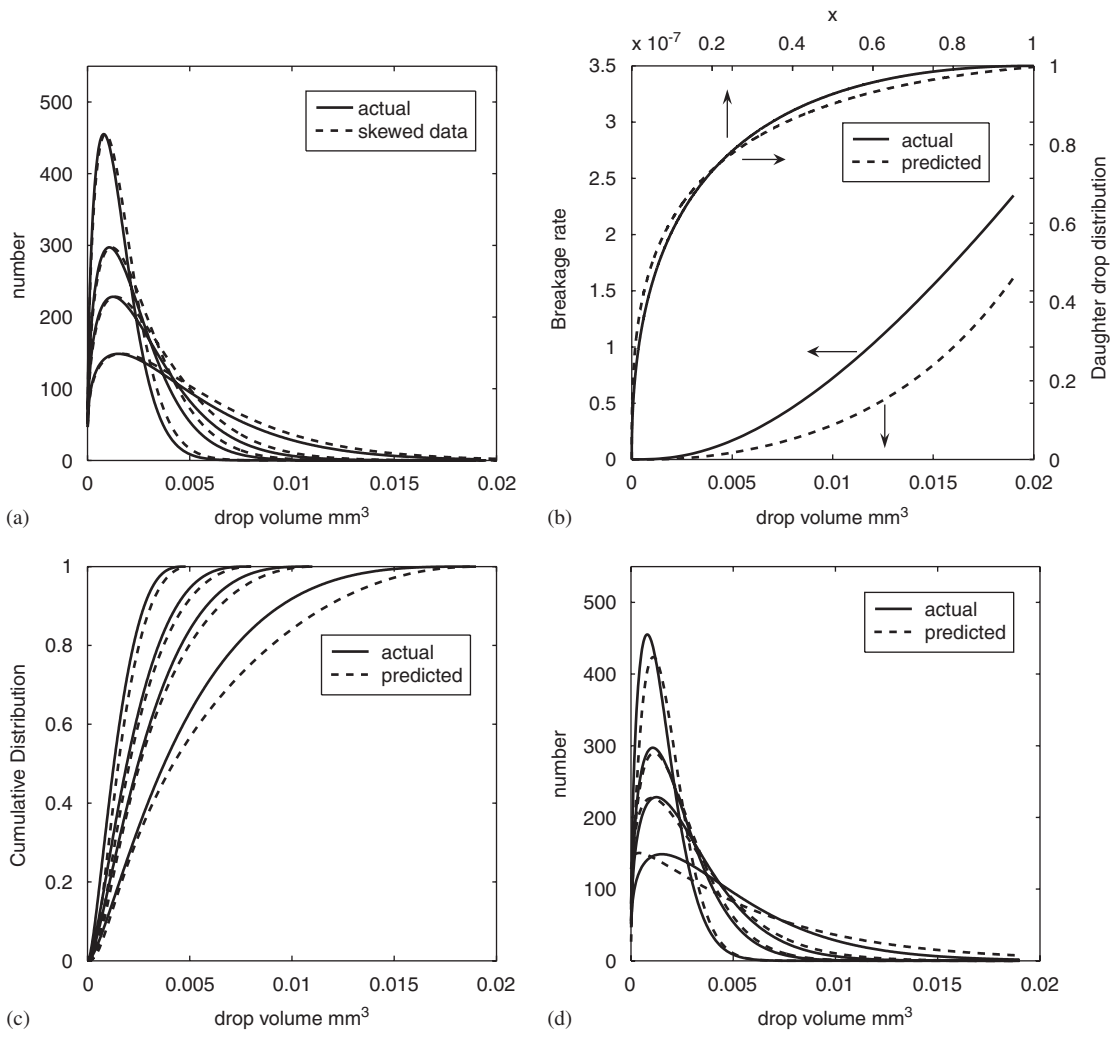


Fig. 5. Inverse population balance modeling results with transient drop volume distributions skewed towards larger drops. (a) Skewed and actual transient number drop distributions. (b) Predicted and actual drop breakage rate and daughter drop distribution functions. (c) Predicted and actual transient cumulative drop distributions. (d) Predicted and actual transient number drop distributions.

the elements $X_{ij}$ can be derived (Sathyagal et al., 1995):

$$X_{ij}=\sqrt{2j}\sum_{k=1}^{n_{\text{term}}}A_k\sum_{m=1}^{j}(-1)^{m-1}\frac{(2j-m)!}{(m-1)!(j-m)!(j-m+1)!}\times\xi_i^{j-m+\mu}\frac{\gamma_c(\alpha_k+m-j-\mu,\beta_k\xi_i)}{\beta^{\alpha_k+m-j-\mu}},\tag{14}$$

where $\gamma_c$ is the complementary incomplete gamma function.

Let the vector $a$ contain the coefficients $a_j$ of the expansion (11) and define the vector $\Phi=\{\Phi_i\}=\xi_i f'(\xi_i)$. Then the inverse problem arising from (10) can be written as: $\Phi = Xa$. This inverse problem is ill-posed in the sense that small changes in the similarity distribution $\xi f'(\xi)$ can induce large changes in the approximated function $\gamma g(x)$. This difficulty is addressed by posing the inverse problem as a least-squares minimization problem:

$$\min_{a\in\Re^{nb}}\|Xa-\Phi\|\tag{15}$$

that is solved subject to the following constraints on the daughter distribution function:

$$g(x)>0,\quad g'(x)\geqslant 0,\quad g'(1)=0.\tag{16}$$

The first two constraints ensure that the distribution function is positive and monotonically increasing. The third constraint results from the assumption that breakup cannot produce daughter drops of near zero volume. The minimization problem equation (15) can be rewritten as

$$\min_{a\in\Re^{nb}}a^{\mathrm{T}}X^{\mathrm{T}}Xa-2a^{\mathrm{T}}X^{\mathrm{T}}\Phi.\tag{17}$$

The least-squares problem (17) is solved by enforcing the constraints (16) at each discretization point $\xi_i$ (Sathyagal et al., 1995).

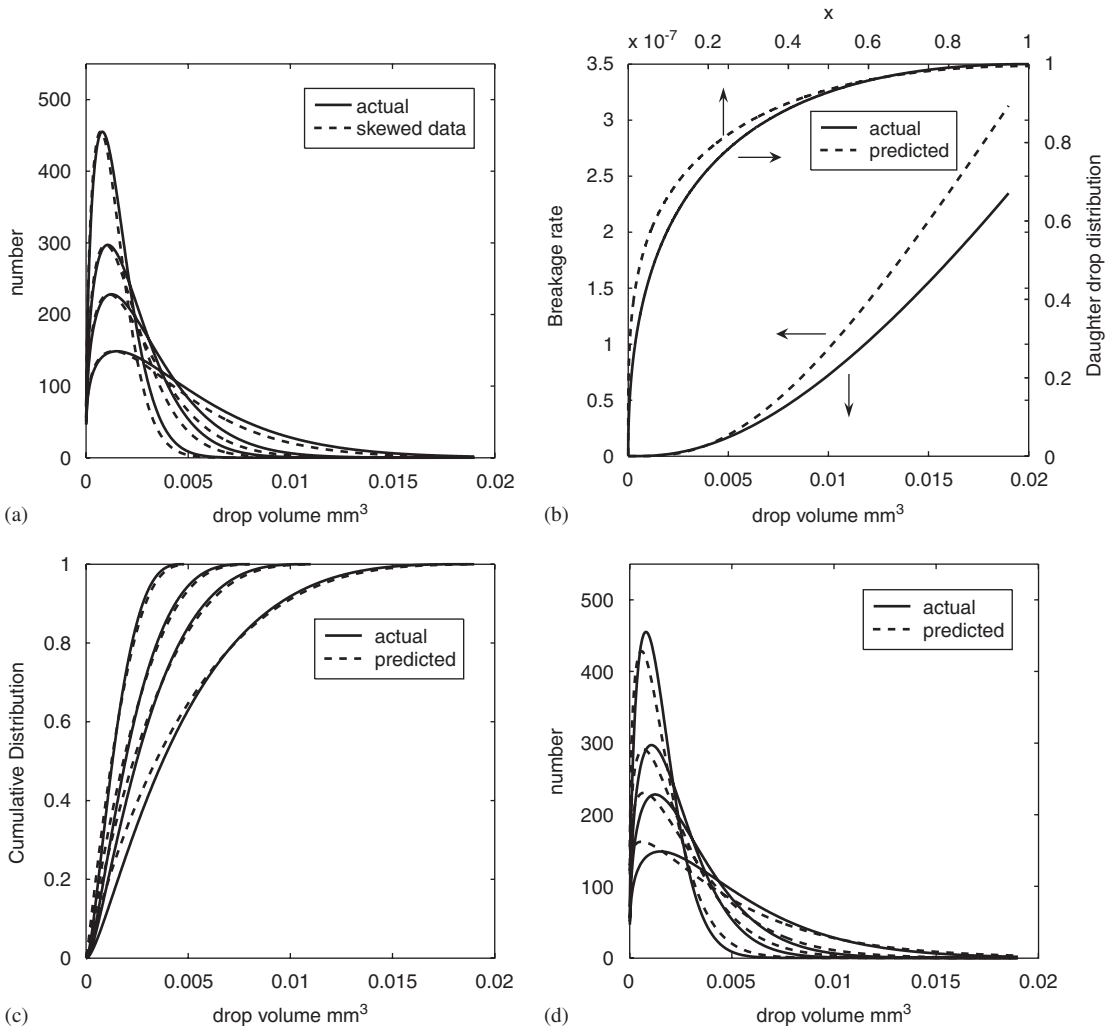


Fig. 6. Inverse population balance modeling results with transient drop volume distributions skewed towards smaller drops. (a) Skewed and actual transient number drop distributions. (b) Predicted and actual drop breakage rate and daughter drop distribution functions. (c) Predicted and actual transient cumulative drop distributions. (d) Predicted and actual transient number drop distributions.

## 4. Simulation results and discussion

The number distribution form of the PBE model (1) was solved numerically by approximating the integral expression using Simpson's Rule with 500 equispaced node points, which was sufficient to obtain a converged solution. This discretization method was used primarily due to its simplicity and ease of implementation. The daughter drop distribution function $G(v, v')$ (4) was converted to the form $\beta(v, v')$ used in the number distribution PBE model. The resulting system of 500 nonlinear ordinary differential equations describing the evolution of the number distribution at each node point $(v_i)$ was solved using Matlab integration code ode45. A single simulation run was used to generate transient drop volume distribution data for the initial coarse distribution:

$$n(v) = \frac{1}{\sigma\sqrt{2\pi}} \exp\left(-\frac{a(v-\mu)^2}{2\sigma^2}\right) = \frac{1}{50\sqrt{2\pi}} \exp[-5000(v-\mu)^2]. \quad (18)$$

Unless otherwise stated, the number distributions at six time points $t = 5, 10, 15, 30, 60$ and 90 min were converted to cumulative distributions for the inverse algorithm (Sathyagal et al., 1995). These time points were chosen to concentrate data at small times when rapid changes were observed and to include a single data point at a large time when the cumulative distribution was changing very slowly. In the subsequent figures, result at only 4 time points are shown for better readability of the plots. For each test presented below, the cumulative distributions were manipulated before being used as input data to the inverse algorithm to mimic various types of measurement errors. Each data was judged to be self-similar by visual inspection of the arc length curves and allowed application of the inversion procedure. The approximate functions for the breakage rate $\Gamma(v)$ and the daughter drop distribution $g(x)$ were compared directly to the actual functions. The impact of measurement errors were further assessed by performing dynamic simulation with the approximate functions and comparing the computed cumulative distributions with the original distributions obtained with the actual functions.

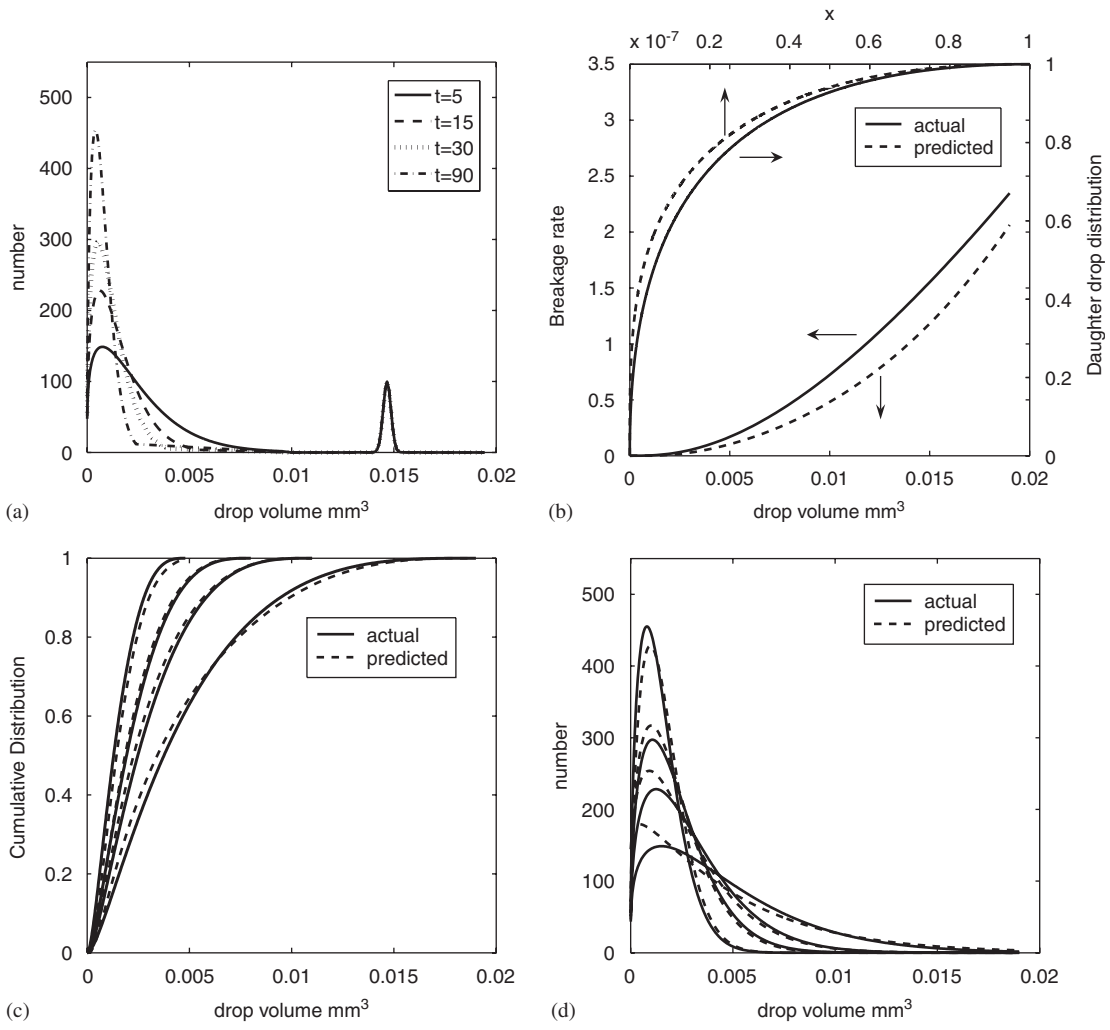


Fig. 7. Inverse population balance modeling results with transient drop volume distributions skewed by dust peak. (a) Skewed transient number drop distributions. (b) Predicted and actual drop breakage rate and daughter drop distribution functions. (c) Predicted and actual transient cumulative drop distributions. (d) Predicted and actual transient number drop distributions.

### *4.1. Perfect data*

We first solved the inverse problem with six unaltered, transient drop volume distributions generated directly from the PBE model. These data were not manipulated by introducing measurement errors and was used to determine the upper limit of estimation performance. The term "perfect data" thus denotes data without any manipulation. Turbulent agitation reduced the mean drop size and produced a more monodispersed emulsion than the original coarse emulsion (Fig. 1(a)). Good approximation results were obtained for both the breakage rate and the daughter distribution function (Fig. 1(b)) over a wide range of drop volumes. PBE model simulation with the approximated functions produced good agreement with the actual cumulative (Fig. 1(c)) and number (Fig. 1(d)) distributions.

We recalculated the cumulative distributions using two other combinations of the breakage and daughter distribution functions to assess the impact of each function on prediction accuracy. When the approximate breakage function was combined with the actual daughter distribution function (Fig. 2(a)), the cumulative distribution ($t = 5$ min) was skewed towards larger drops for small drop volumes and skewed towards smaller drops for large drop volumes. These errors were a direct result of the breakage rate (Fig. 1(b)), which was slightly underestimated for small drop volumes and overestimated for large drop volumes. When the approximate distribution function was combined with the actual breakage function (Fig. 2(b)), the cumulative distribution was skewed towards smaller drops for small drop volumes. This trend was caused by the distribution function being skewed towards smaller $x$ values (Fig. 1(b)), which corresponds to a larger distribution of small drops.

The interpretation of results is more complicated when both approximate functions were used to generate the cumulative distributions, which is the case of primary interest. The individual errors obtained with the approximate breakage function (Fig. 2(a)) and the approximate distribution function (Fig. 2(b)) were largely cancelled when the approximate functions were combined to generate the final distribution (Fig. 2(c)). However,

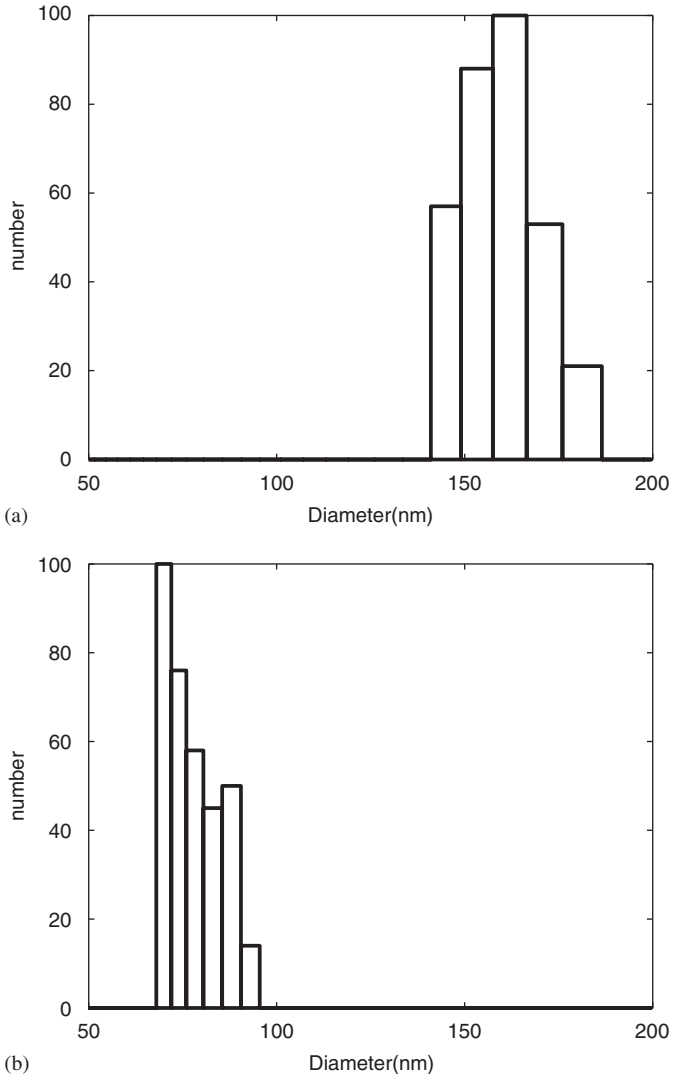


Fig. 8. Drop size distribution measurements obtained with dynamic light scattering for a mineral oil in water emulsion with Pluronic F-68 as the surfactant. (a) Results for a coarse emulsion obtained with a stator–rotor device. (b) Results for a processed emulsion obtained with a single pass of a high-pressure homogenizer.

the effects of the approximation errors were more evident in the transient prediction (Figs. 1(c), (d)). The distributions were skewed towards smaller drops at small times due to underprediction of the distribution function, while they were skewed towards larger drops at large times due to underprediction of the breakage rate.

### 4.2. Noisy data

To investigate the impact of measurement noise, we corrupted the drop volume distribution data with artificial noise as follows:

$$\bar{n}(v,t) = n(v,t) + v(r-0.5)n(v,t), \tag{19}$$

where $n(v,t)$ is the number distribution data obtained with the actual functions (see Fig. 1(a)), $r$ is a random number between 0 and 1, $v = 0.3$ and $\bar{n}(v,t)$ is the noisy number distribution data used to generate the input data for the inverse algorithm. We utilized uniform rather than normal noise to ensure that the noisy data $\bar{n}(v,t)$ remained positive, which is expected from any measurement device.

First we solved the inverse problem with six cumulative distributions generated from the noisy number distributions at $t = 5, 10, 15, 30, 60,$ and 90 min (Fig. 3(a)). Fig. 4(a) shows the associated cumulative distributions. The noisy cumulative distributions had fewer large drops than the noise-free distributions, leading to underestimation of the breakage rate at large drop volumes (Fig. 3(b)). More difficult to explain was the behavior of the daughter distribution function, which produced a larger number distribution of small drops and a smaller number distribution of large drops than the actual function (Fig. 3(b)). These approximation errors were manifested in the predicted cumulative (Fig. 3(c)) and number (Fig. 3(d)) distributions. Both functions were important at short times, thereby yielding overprediction of small drops and underprediction of very large drops. At longer times the breakage rate became dominant, and a larger proportion of large drops was predicted compared to the original noise-free data.

We repeated the noisy data test with twelve cumulative distributions generated from the noisy number distributions at $t = 5, 7.5, 10, 12.5, 15, 22.5, 30, 45, 60, 75, 90$ and 105 min with the expectation that more transient data would improve the function approximation results. The daughter distribution function was significantly improved, while the breakage rate was slightly degraded (Fig. 4(b)). Consequently, only modest improvements in transient distribution predictions at short times were obtained (Figs. 4(c), (d)). Because the noisy cumulative distributions were skewed towards smaller drops, these results suggest that the collection of more transient data will prove largely ineffective if the data are uniformly skewed.

### 4.3. Skewed data

Available technologies such as dynamic light scattering (e.g. Schmitz, 1990) have a tendency to skew measured drop size distributions. To examine the impact of such measurement errors, we skewed the drop volume distribution data as follows:

$$\bar{n}(v,t) = n(\bar{v},t), \quad \bar{v} = v \pm \delta v, \tag{20}$$

where $n(v,t)$ is the number distribution data obtained with the actual functions (Fig. 1(a)), $\bar{v}$ is the skewed volume. $\delta$ determines the amount of skewness, the sign determines the direction of skewness, either towards smaller drops (negative) or larger drops (positive), and $\bar{n}(v,t)$ is the skewed distribution. Skewed distributions at $t = 5, 10, 15, 30, 60,$ and 90 min were used as input data to the inverse algorithm.

First, we examined skewing towards larger drops with $\delta = +0.0005$, which produced number distributions that increasingly deviated from the original distributions at large drop volumes (Fig. 5(a)). Substantial underestimation of the breakage rate was observed, while only small errors were obtained in the daughter distribution function (Fig. 5(b)). The predicted

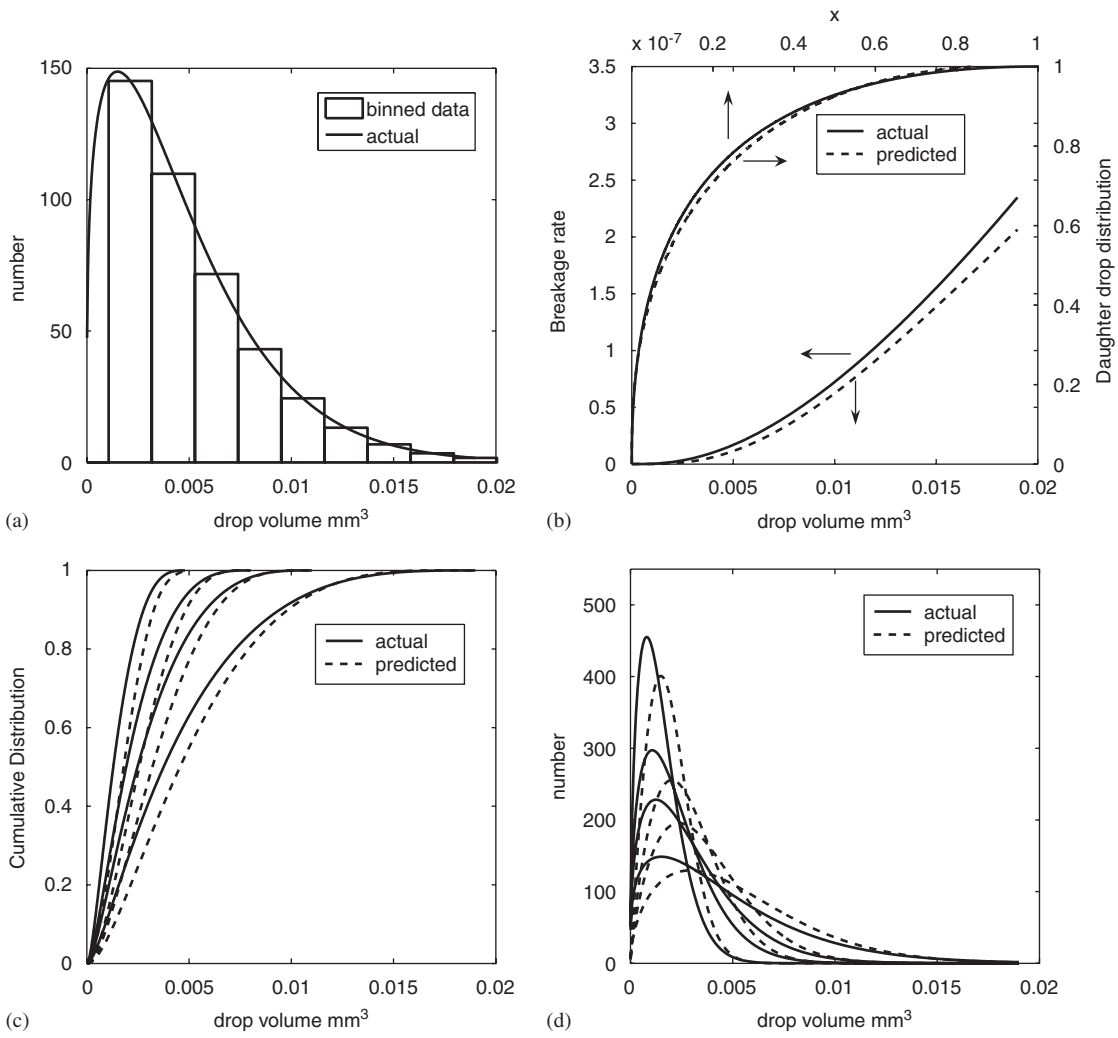


Fig. 9. Inverse population balance modeling results with transient drop volume distributions represented by 10 bins. (a) The binned transient number drop distribution at $t = 5$ min. (b) Predicted and actual drop breakage rate and daughter drop distribution functions. (c) Predicted and actual transient cumulative drop distributions. (d) Predicted and actual transient number drop distributions.

cumulative distributions consistently trailed the actual distributions (Fig. 5(c)) in that the number of large drops was generally overpredicted. This behavior is easily interpreted from the number distribution predictions (Fig. 5(d)), which show an overprediction of small drops at small times and a consistent overprediction of large drops.

Next, the number distributions were skewed towards smaller drops with $\delta = -0.0005$. Because the number distributions were more skewed towards small drops at large drop volumes (Fig. 6(a)), the breakage rate function only agreed with the actual function at very small drop volumes (Fig. 6(b)). Interestingly, the daughter distribution was significantly underestimated except at large drop volumes where the data was most skewed (Fig. 6(b)). The predicted cumulative distributions led the actual distributions until the approximate breakage function approached the actual function at large times (Fig. 6(c)). The predicted number distributions produced a larger number of small drops than the actual distributions (Fig. 6(d)), which was consistent with overprediction of the breakage rate.

### 4.4. Dust particles

Drop size distribution measurements produced by dynamic light scattering are sensitive to contaminants such as dust particles that create artificial peaks at large drop sizes (Schmitz, 1990). For emulsions, dust particles are not easily removed by filtering because shearing can cause drop breakage. While dust peaks can be eliminated by restricting the size range analyzed, this approach requires a priori knowledge about the drop size distribution. Therefore, we investigated the effect of artificial peaks in the number distribution data at large drop volumes. For simplicity, a single peak was assumed to be normally distributed about a large drop volume and to remain constant with time (Fig. 7(a)). This peak caused significant underestimation of the breakage rate (Fig. 7(b)) and produced a daughter distribution that predicted a larger proportion of small drops (Fig. 7(b)). The tradeoff between these two errors was evident in the predicted cumulative (Fig. 7(c)) and number (Fig. 7(d)) distributions, where the daughter distribution

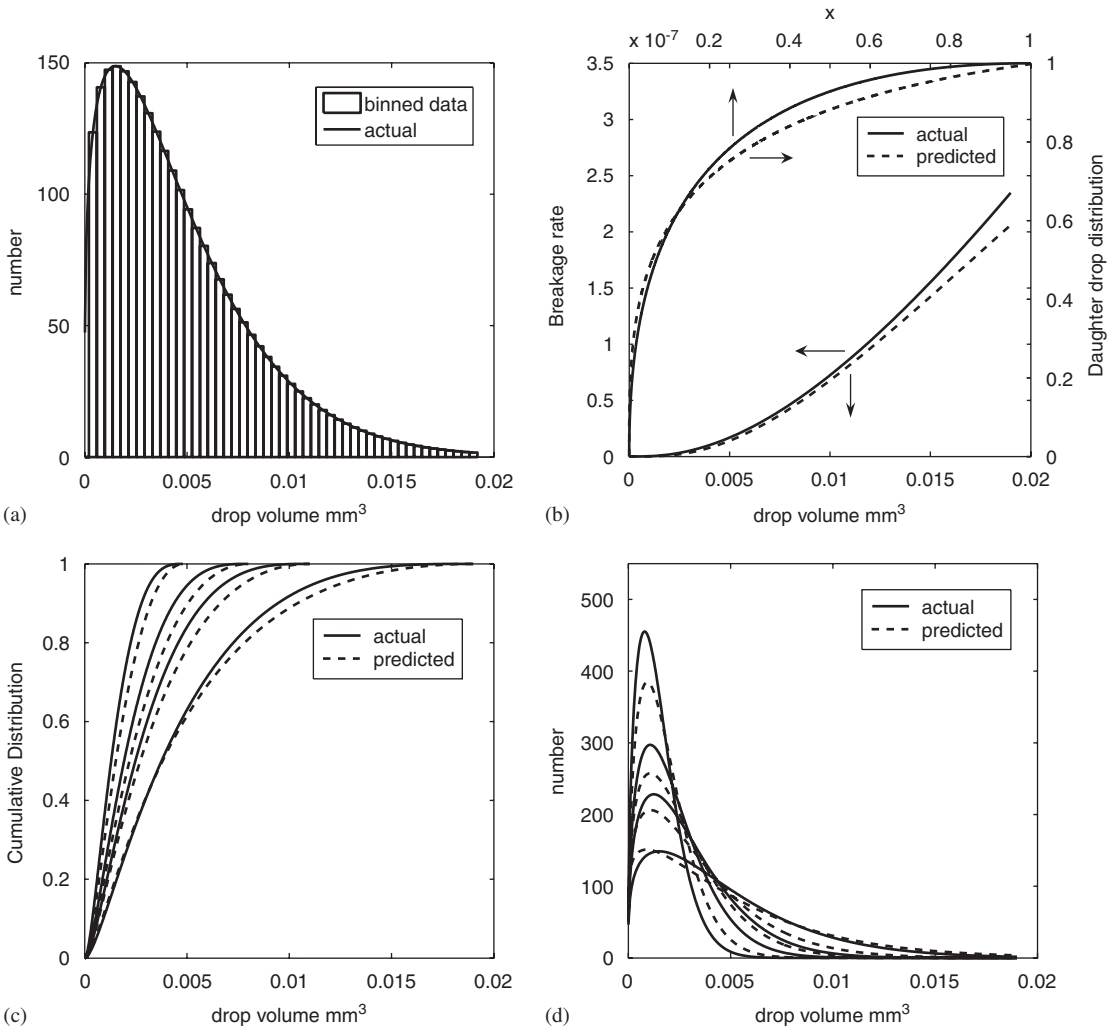


Fig. 10. Inverse population balance modeling results with transient drop volume distributions represented by 50 bins. (a) The binned transient number drop distribution at $t = 5$ min. (b) Predicted and actual drop breakage rate and daughter drop distribution functions. (c) Predicted and actual transient cumulative drop distributions. (d) Predicted and actual transient number drop distributions.

function was dominant for small drop volumes and the breakage rate function was dominant for large drop volumes. The breakage function became dominant at longer times when the predicted distributions trailed the actual distributions due to underestimation of drop breakage.

### 4.5. Binned data

In the previous simulation tests, the distribution data was essentially a continuous function of the drop volume due to the large number (500) of node points used for numerical solution. By contrast, drop size distributions measured by dynamic light scattering (DLS) have limited resolution due to binning operations. We have used DLS (Brookhaven Instruments) to measure drop size distributions for mineral oil ($\approx 0.04$ wt%) in water emulsions with Pluronic F-68 ($\approx 0.008$ wt%) as the surfactant. Initial coarse emulsions prepared using a stator–rotor device (*Ultra-Turrax*, *T 25 basic*, IKA Works, Inc.) were introduced to a high pressure homogenizer (*Emulsiflex C-3*, Avestin, Inc.) operated at 25,000 psig. The mean and variance of the coarse drop size distribution (Fig. 8(a)) were significantly reduced by a single homogenization pass (Fig. 8(b)). However, the instrument produced low resolution distributions due to the small number of bins used.

We conducted a final set of simulation tests to investigate the impact of drop size binning on the inverse algorithm. Number drop distributions were used as input data by holding the distribution constant at the mean volume across each bin. Each number distribution was converted to a cumulative distribution from which volume values were interpolated to generate the $\ln t$ vs $\ln v$ plots. Then the inversion procedure was implemented as described earlier. Initially, 10 bins were used to mimic the DLS experimental results (Fig. 9(a)). The breakage rate was underestimated at large drop volumes, and the daughter distribution function exhibited errors at intermediate volumes (Fig. 9). Consequently, the predicted cumulative distributions (Fig. 9(c)) trailed the actual continuous distributions. The number distributions (Fig. 9(d)) showed that a greater number

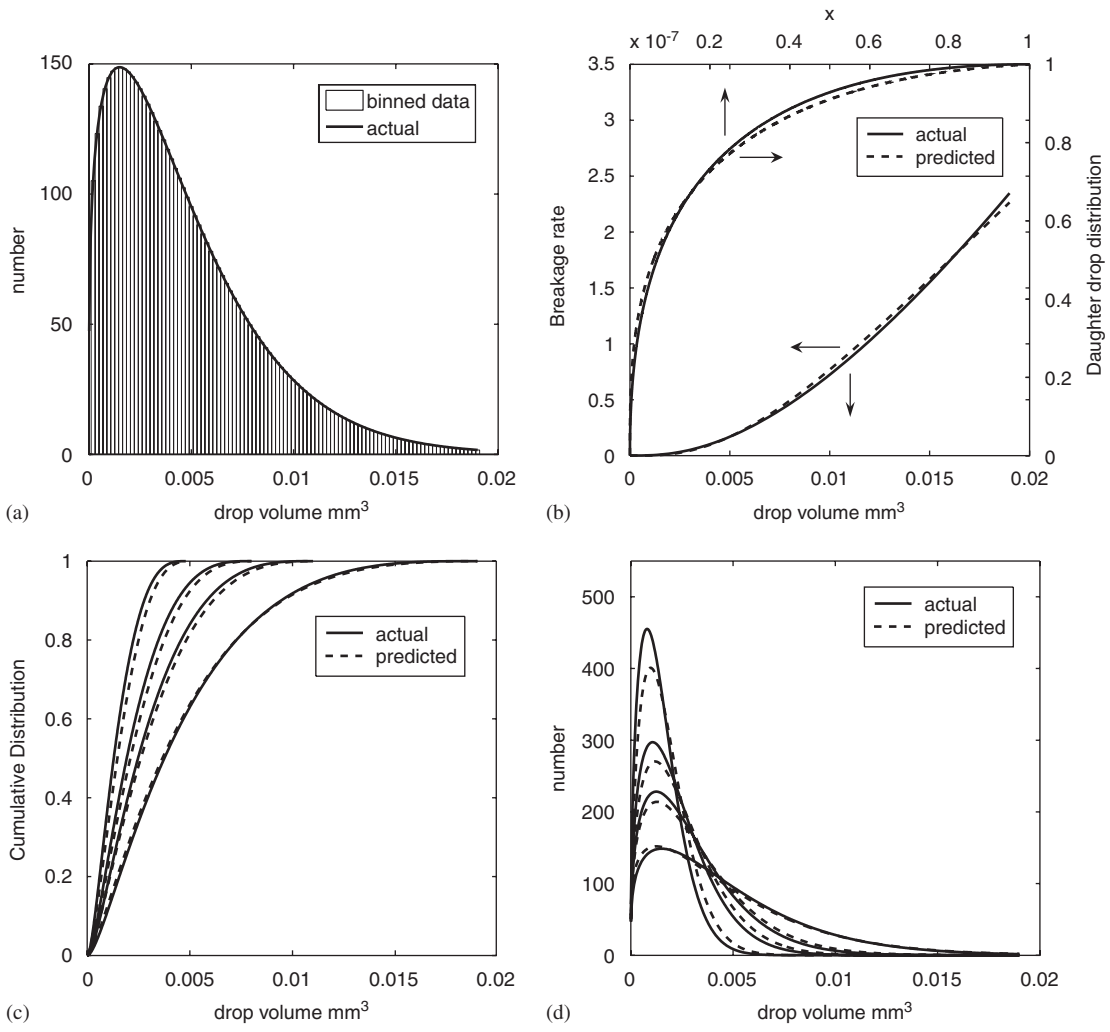


Fig. 11. Inverse population balance modeling results with transient drop volume distributions represented by 200 bins. (a) The binned transient number drop distribution at $t = 5$ min. (b) Predicted and actual drop breakage rate and daughter drop distribution functions. (c) Predicted and actual transient cumulative drop distributions. (d) Predicted and actual transient number drop distributions.

of large drops are predicted due to the underestimation of the breakage rate.

We repeated the test with 50 bins to determine if the continuous data results could be recovered (Fig. 10). While the breakage rate was estimated slightly more accurately than with 10 bins, the daughter distribution function exhibited larger errors at large drop volumes (Fig. 10). As a result, the predicted cumulative distributions (Fig. 10(c)) were only slightly improved compared to ten bins (Fig. 9) and significantly degraded compared to continuous data (Fig. 1). The number distributions (Fig. 10(d)) showed underprediction of small drops and overprediction of large drops, especially at long times. To validate the binning procedure, we repeated the test with 200 bins (Fig. 11). The breakage rate and daughter distribution functions (Fig. 11), the cumulative distributions (Fig. 11(c)), and the number distributions (Fig. 11(d) compared favorably to those obtain with continuous data (Fig. 1). Very close agreement was obtained when 500 bins were used (results not shown). Taken together, these results suggest that the inverse method can be rather sensitive to data binning.

## 5. Conclusions and future work

We investigated the impact of measurement errors in transient particle size distributions on the inverse PBE modeling method of Ramkrishna and co-workers. A previously published model of liquid–liquid dispersion drop volume evolution in a turbulently agitated batch vessel was used to generate transient distribution data, which were subjected to various types of errors before being used as input data to the inverse algorithm. The quality of the inversion results were assessed by comparing the estimated breakage rate and daughter distribution functions, as well as predicted distributions, to the original model.

We found that most errors considered degraded estimation of the breakage rate function at large drop volumes, presumably due to the limited data available for large drops in the transient distributions used as input data. The daughter distribution

function also exhibited significant errors for most of the cases considered. However, the breakage function, and to a lesser extent the distribution function, often showed good agreement with the actual functions at small drop volumes. Consequently, predicted distributions tended to be more accurate at longer times when there was a preponderance of small drops due to repeated breakage. Our results suggest that the inverse algorithm can generate PBE functions that allow sufficiently accurate prediction of final drop size distributions despite errors in measured distributions used as input data.

Our long-term goal is to develop inverse-based methods for extracting PBE model functions of emulsion drop breakage and coalescence in high-pressure homogenization. This future work will require modification of the inverse method presented because homogenization is not properly modeled as a well-mixed, batch process. However, the sensitivity analysis techniques presented in this paper will provide a suitable framework for assessing the impact of distribution measurement errors on the inversion procedure. These modeling and analysis studies will be reported in our future publications.

## References


Abramowitz, M., Stegun, A., 1964. Handbook of Mathematical Functions with Formulas, Graphs, and Mathematical Tables. National Bureau of Standards. Applied Mathematics Series, vol. 55. Washington, DC.

Alexopoulos, A., Kiparissides, C., 2005. Part II: Dynamic evolution of the particle size distribution in particulate processes undergoing simultaneous particle nucleation, growth and aggregation. Chemical Engineering Science 60 (15), 4157–4169.

Alexopoulos, A., Roussos, A., Kiparissides, C., 2004. Part I: Dynamic evolution of the particle size distribution in particulate processes undergoing combined particle growth and aggregation. Chemical Engineering Science 59 (24), 5751–5769.

Alopaeus, V., Koskinen, J., Keskinen, K., 1999. Simulation of the population balances for liquid–liquid systems in a nonideal stirred tank. Part 1. Description and qualitative validation of the model. Chemical Engineering Science 54 (24), 5887–5899.

Alopaeus, V., Koskinen, J., Keskinen, K., Majander, J., 2002. Simulation of the population balances for liquid–liquid systems in a nonideal stirred tank. Part 2—Parameter fitting and the use of the multiblock model for dense dispersions. Chemical Engineering Science 57 (10), 1815–1825.

Alopaeus, V., Koskinen, J., Keskinen, K., 2003. Utilization of population balances in simulation of liquid–liquid systems in mixed tanks. Chemical Engineering Communications 190 (11), 1468–1484.

Becher, P., 1983. Encyclopedia of Emulsion Technology, vol. 1. Marcel Dekker, New York, NY.

Becher, P., 2001. Emulsions: Theory and Practice. Oxford University Press, New York, NY.

Chen, Z., Pruss, J., Warnecke, H., 1998. A population balance model for disperse systems: drop size distribution in emulsion. Chemical Engineering Science 53 (5), 1059–1066.

Coulaloglou, C., Tavlarides, L., 1977. Description of interaction processes in agitated liquid–liquid dispersions. Chemical Engineering Science 32 (11), 1289–1297.

Floury, J., Bellettre, J., Legrand, J., Desrumaux, A., 2004a. Analysis of a new type of high pressure homogeniser: a study of the flow pattern. Chemical Engineering Science 59 (4), 843–853.

Floury, J., Legrand, J., Desrumaux, A., 2004b. Analysis of a new type of high pressure homogeniser: Part b: Study of droplet break-up and recoalescence phenomena. Chemical Engineering Science 59 (6), 1285–1294.

Kostoglou, M., Karabelas, A., 1997. An explicit relationship between steady-state size distribution and breakage kernel for limited breakage processes. Journal of Physics A—Mathematical and General 30 (20), L685–L691.

Kostoglou, M., Karabelas, A., 2001. A contribution towards predicting the evolution of droplet size distribution in flowing dilute liquid/liquid dispersions. Chemical Engineering Science 56 (14), 4283–4292.

Kostoglou, M., Karabelas, A., 2005. On the self-similar solution of fragmentation equation: numerical evaluation with implications for the inverse problem. Journal of Colloid and Interface Science 284 (2), 571–581.

Kostoglou, M., Dovas, S., Karabelas, A., 1997. On steady-state size distribution of dispersions in breakage process. Chemical Engineering Science 52 (8), 1285–1299.

Kumar, S., Ramkrishna, D., 1996a. On the solution of population balance equations by discretization 1. A fixed pivot technique. Chemical Engineering Science 51 (8), 1311–1332.

Kumar, S., Ramkrishna, D., 1996b. On the solution of population balance equations by discretization 2. A moving pivot technique. Chemical Engineering Science 51 (8), 1333–1342.

Maguire, L., Zhang, H., Shamlou, P., 2003. Preparation of small unilamellar vesicles (SUV) and biophysical characterization of their complexes with poly-L-lysine-condensed plasmid DNA. Biotechnology and Applied Biochemistry 37, 73–81.

Mahoney, A., Doyle, F., Ramkrishna, D., 2002. Inverse problems in population balances: growth and nucleation from dynamic data. A.I.Ch.E. Journal 48 (5), 981–990.

Malmsten, M., 2002. Surfactants and Polymers in Drug Delivery. Marcel Dekker, Inc., New York.

Marti-Mestres, G., Nielloud, F., 2002. Emulsions in health care applications—An overview. Journal of Dispersion Science and Technology 23 (1–3), 419–439.

Narsimhan, G., Ramkrishna, D., Gupta, J., 1980. Analysis of drop size distributions in lean liquid–liquid dispersions. A.I.Ch.E. Journal 26 (6), 991–1000.

Narsimhan, G., Nejfelt, G., Ramkrishna, D., 1984. Breakage functions for droplets in agitated liquid–liquid dispersions. A.I.Ch.E. Journal 30 (3), 457–467.

Nielloud, F., Marti-Mestres, G., 2000. Pharmaceutical Emulsions and Suspensions. Marcel Dekker, Inc., New York, NY.

Ramkrishna, D., 1974. Drop-breakage in agitated liquid–liquid dispersions. Chemical Engineering Science 29 (4), 987–992.

Ramkrishna, D., 2000. Population Balances: Theory and Applications to Particulate Processes in Engineering. Academic Press, New York, NY.

Ramkrishna, D., Mahoney, A., 2002. Population balance modeling: promise for the future. Chemical Engineering Science 57 (4), 595–606.

Ramkrishna, D., Sathyagal, A., Narsimhan, G., 1995. Analysis of dispersed-phase systems—fresh perspective. A.I.Ch.E. Journal 41 (1), 35–44.

Ruiz, M., Padilla, R., 2004. Analysis of breakage functions for liquid–liquid dispersions. Hydrometallurgy 72 (3–4), 245–258.

Ruiz, M., Lermanda, P., Padilla, R., 2002. Drop size distribution in a batch mixer under breakage conditions. Hydrometallurgy 63 (1), 65–74.

Sathyagal, A., Ramkrishna, D., 1996. Droplet breakage in stirred dispersions: breakage functions from experimental drop-size distributions. Chemical Engineering Science 51 (9), 1377–1391.

Sathyagal, A., Ramkrishna, D., Narsimhan, G., 1995. Solution of inverse problems in population balances 2: particle break-up. Computers & Chemical Engineering 19 (4), 437–451.

Schmitz, K.S., 1990. Dynamic Light Scattering by Macromolecules. Academic Press, San Diego.

Simon, M., Schmidt, S., Bart, H., 2003. The droplet population balance model—Estimation of breakage and coalescence. Chemical Engineering and Technology 26 (7), 745–750.

Soon, S., Harbidge, J., Titchener-Hooker, N., Shamlou, P., 2001. Prediction of drop breakage in an ultra high velocity jet homogenizer. Journal of Chemical Engineering of Japan 34 (5), 640–646.

Sovova, H., 1981. Breakage and coalescence of drops in a batch stirred vessel. 2. Comparison of model and experiments. Chemical Engineering Science 36 (9), 1567–1573.

Sovova, H., Prochazka, J., 1981. Breakage and coalescence of drops in a batch stirred vessel. 1. Comparison of continuous and discrete models. Chemical Engineering Science 36 (1), 163–171.

Tsouris, C., Tavlarides, L., 1994. Breakage and coalescence models for drops in turbulent dispersions. A.I.Ch.E. Journal 40 (3), 395–406.

Walstra, P., 1993. Principles of emulsion formation. Chemical Engineering Science 48 (2), 333–349.

Wang, T., Wang, J., Jin, Y., 2006. A CFD-PBM coupled model for gas–liquid flows. A.I.Ch.E. Journal 52 (1), 125–140.

Wright, H., Ramkrishna, D., 1992. Solutions of inverse problems in population balances. 1: Aggregation kinetics. Computers and Chemical Engineering 16 (12), 1019–1038.